Primary pulmonary malignant melanoma with H3K27Me3 loss: A case report

HOUQIANG LI[1-3*], LANQING ZHENG[2,4*], XUNBIN YU[1-3], LINFENG CHEN[1-3], SHANSHAN LV[1-3] and XIN CHEN[1-3]

[1]Department of Pathology, Fuzhou University Affiliated Provincial Hospital, Fuzhou, Fujian 350001, P.R. China; [2]Shengli Clinical Medical College of Fujian Medical University, Fuzhou, Fujian 350001, P.R. China; [3]Department of Pathology, Fujian Provincial Hospital, Fuzhou, Fujian 350001, P.R. China; [4]Department of Nursery, Fujian Provincial Hospital, Fuzhou, Fujian 350001, P.R. China

Received November 1, 2024; Accepted Marhc 7, 2025

DOI: 10.3892/ol.2025.15084

Abstract. Primary pulmonary malignant melanoma (pPMM) is an exceptionally rare type of primary malignant tumor. The present study reports a unique case of pPMM in a 54-year-old woman. Surgical resection revealed a tumor localized around the bronchus, showing nodular growth with relatively well-defined borders and no evidence of local or distant metastasis. To further characterize this rare pPMM, histological analysis, immunohistochemistry, sanger sequencing and next-generation sequencing were conducted. Histologically, the tumor exhibited biphasic differentiation, with both epithelial-like and spindle cell-like features, as well as high-grade characteristics, including significant atypia, necrosis and a high mitotic index. Key diagnostic features of malignant melanoma were evident, including prominent red nucleoli and melanin pigmentation. Immunohistochemistry confirmed the presence of melanoma markers and demonstrated a loss of H3K27Me3 expression. The programmed death-ligand 1 positivity rate of the tumor was 60%. NGS identified a mutation in the *TP53* and *NTRK3* genes, but no *BRAF* mutation was detected. This case report highlights the unique presentation of pPMM with H3K27Me3 loss and provides insights into its genomic profile, pathogenesis and natural history.

Introduction

Malignant melanoma (MM) is primarily a highly aggressive non-epithelial tumor affecting skin tissue. Patients often have a history of skin melanocytic nevi and may present with cutaneous ulcerations. Although MM is typically associated with the skin, it can also occur in other sites, including the esophagus, oral cavity, anus and vagina (1). The clinical diagnosis of MM typically relies on histopathological examination and immunohistochemical markers such as sry-box transcription factor 10 (SOX10), melan-A and human melanoma black-45 (HMB-45), which are essential for differentiating it from other malignancies. Primary pulmonary malignant melanoma (pPMM) is an extremely rare manifestation, accounting for ~0.001% of primary malignant lung tumors and 0.4% of all malignant melanomas (1). Due to its rarity, pPMM poses diagnostic challenges and is often misdiagnosed as other malignancies, such as malignant peripheral nerve sheath tumors (MPNSTs) or metastatic melanoma. The absence of a cutaneous or mucosal primary site further complicates the diagnostic process. H3K27Me3 is a post-translational modification associated with transcriptional repression and tumor suppressor gene silencing (2). Loss of H3K27Me3 has been implicated in the progression of various aggressive tumors, such as MPNSTs and glioblastoma (2,3). The present study discusses a unique case of pPMM characterized by H3K27Me3 loss, examining its genomic profile, pathogenesis and natural history, along with relevant literature. Notably, this case was initially misdiagnosed as a MPNST based on overlapping histopathological and immunohistochemical features. This case underscores the challenges in diagnosing rare malignancies, particularly when they mimic more common entities. The case highlights the importance of comprehensive histological, immunohistochemical and molecular evaluations in achieving a definitive diagnosis, especially in cases with overlapping features.

Case report

Patient. The patient, a 54-year-old woman with no prior history of skin, ear, or eye lesions, presented to Fujian Provincial Hospital (Fuzhou, China) in November 2017 with symptoms of chest tightness and 2.5 kg of weight loss, although no cough, chest pain or hemoptysis were reported. At 8 months prior to lobectomy, a computed tomography scan

Correspondence to: Dr Houqiang Li, Department of Pathology, Fuzhou University Affiliated Provincial Hospital, 134 East Street, Gulou, Fuzhou, Fujian 350001, P.R. China
E-mail: docli254@163.com

*Contributed equally

Key words: malignant melanoma, pulmonary, H3K27Me3, genomic analysis, programmed death-ligand 1

revealed a 4.1x2.3-cm mass in the basal segment of the right lower lung lobe, suggesting a possible lesion. No treatment was initiated at that time. After 5 months, a follow-up scan showed the mass had grown to 5.0x2.9 cm, with irregular borders and high metabolic activity on positron emission tomography-computed tomography, which raised suspicion of a malignant mesenchymal tumor (Fig. 1). A lobectomy was subsequently performed, during which laparoscopic exploration revealed no adhesions or effusions. The mass involved the lung capsule but without any enlarged lymph nodes.

Pathological examination. The resected lung lobe specimen showed a nodular mass measuring 3x2.8x2.5 cm, located 1.5 cm from the lung capsule. The mass was unencapsulated, with a well-defined border and a delicate grayish-white texture on the cut surface. Histological analysis was performed on tissue sections fixed in 10% neutral buffered formalin at room temperature for 24 h. The tissue was processed, embedded in paraffin and sectioned at a thickness of 5 μm. Sections were stained with hematoxylin and eosin at room temperature, following standard protocols. The slides were examined using a light microscope (Leica DM3000) at magnifications of x100, x200 and x400, and scale bars were included in the figure legends for reference. The analysis revealed a nodular tumor with infiltrative growth and biphasic differentiation, consisting of epithelioid and spindle-shaped cells (Fig. 2A). The epithelioid cell region displayed marked cellular atypia with pleomorphic nuclei and eosinophilic cytoplasm (Fig. 2B), while the spindle cell region showed whorl-like structures and hyaline degeneration of the interstitium (Fig. 2C). Tumor cells exhibited bizarre appearances (Fig. 2D) and transparent cytoplasm (Fig. 2E). The mitotic rate was 12 mitoses per 10 high-power fields, with frequent necrosis and melanin accumulation (Fig. 2F). Extensive fibrous stroma was present, with infiltrating lymphocytes, plasma cells and eosinophils. The residual bronchial mucosa showed no significant atypia, but scattered or nest-like melanoma cells were observed infiltrating beneath the bronchial mucosal epithelium without ulceration present (Fig. 2G).

Immunophenotype and genomic assessment. Immunohistochemistry (IHC) staining was performed on 4-μm sections obtained from the formalinfixed paraffinembedded tissues using automated immunostainers. The IHC automated staining protocol was performed as described previously (4). The detailed information on the immunohistochemical experiments has been provided in Table SI, including the concentrations of reagents, suppliers, product catalog numbers, incubation conditions (temperature and duration). PBS was used as the negative control. The tumor cells expressed melanoma markers, including S-100 (data not shown), SOX10 (Fig. 3A), melan-A (Fig. 3B), HMB-45 and microphthalmia-associated transcription factor (data not shown), with stronger expression in the epithelioid regions compared with that in the spindle cell regions. Immunohistochemical staining for H3K27Me3 was negative in the tumor cells (Fig. 3C). The Ki-67 proliferation index was ~70%, and the programmed death-ligand 1 (PD-L1) (SP263) positivity rate was 60% (Fig. 3D). Other markers, including BRAF, neurotrophic tyrosine receptor kinase (NTRK), transcription factor e3, AE1/AE3, epithelial membrane antigen (EMA), anaplastic lymphoma kinase (ALK), CD34, smooth muscle actin (SMA), desmin, thyroid transcription factor-1 (TTF1) and Napsin-A, were negative.

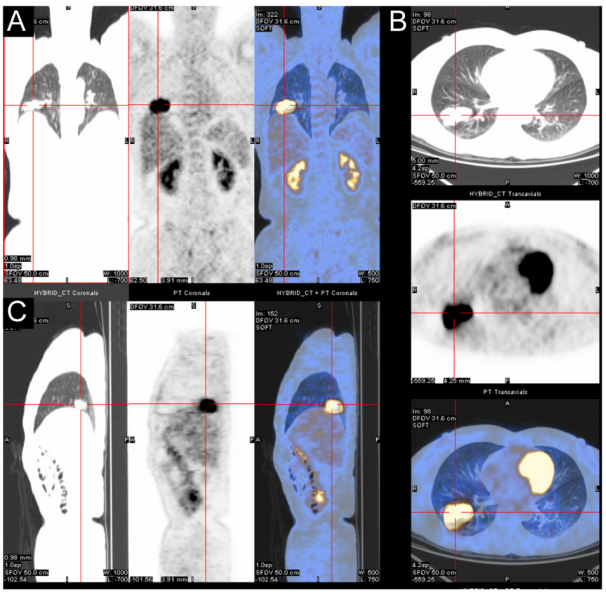

Figure 1. Multi-slice and multi-view display of fused computed tomography and positron emission tomography-computed tomography scan images. (A) Anteroposterior, (B) axial fused and (C) lateral images.

The Next-generation sequencing (NGS) assay was conducted using a laboratory developed test kit from Amoy Diagnostics, Co., Ltd., which was designed to sequence the entire coding regions of 116 cancer-relate genes. Raw sequencing reads were converted into FastQ files using bcl2fastq (Illumina), enabling reliable downstream analysis. The platform enables the detection of various classes of genomic alterations, including point mutations, indel, gene fusions and copy number variations. The NGS protocol was implemented as described previously (5). The NGS identified four somatic mutations, namely *TP53*, *BCL2L11*, *NF1* and *NTRK3*. Among them, *TP53* is significant for targeted therapeutics (Fig. 3E; Table I). *BRAF* and *KIT* mutations, typically associated with skin melanoma, were not identified.

Follow-up. After several days of postoperative recovery, the patient was scheduled for follow-up visits every 3 months for the first 3 years. Due to financial constraints, the patient opted out of further therapy. Currently, at 72 months post-surgery, the patient is on a favorable recovery trajectory, showing no evidence of disease.

Discussion

MM, typically a highly aggressive tumor, is predominantly found in the skin. Patients often present with a history of melanocytic nevi and may have skin ulcerations. Although PMM is usually metastatic from skin lesions (6), pPMM is exceptionally rare. The median age of diagnosis is ~59.1 years, with no significant sex differences reported. Unlike for numerous lung cancers, smoking is not considered a risk factor for pPMM. Most cases are incidentally discovered during routine physical

Table I. Somatic mutation identified by the next-generation sequencing.

Gene	Detection result [accession number]	Abundance/copy number, %
TP53	exon6 c.658T>C p. (Y220H) [NM_000546.5]	30.03
NTRK3	exon3 c.148G>A p. (D50N) [NM_002530.4]	60.73
BCL2L11	intron2c.394+1479_394+4381del [NM_138621.5]	28.98
NF1	exon3c.266C>G p. (T89R) [NM_001042492.3]	8.40

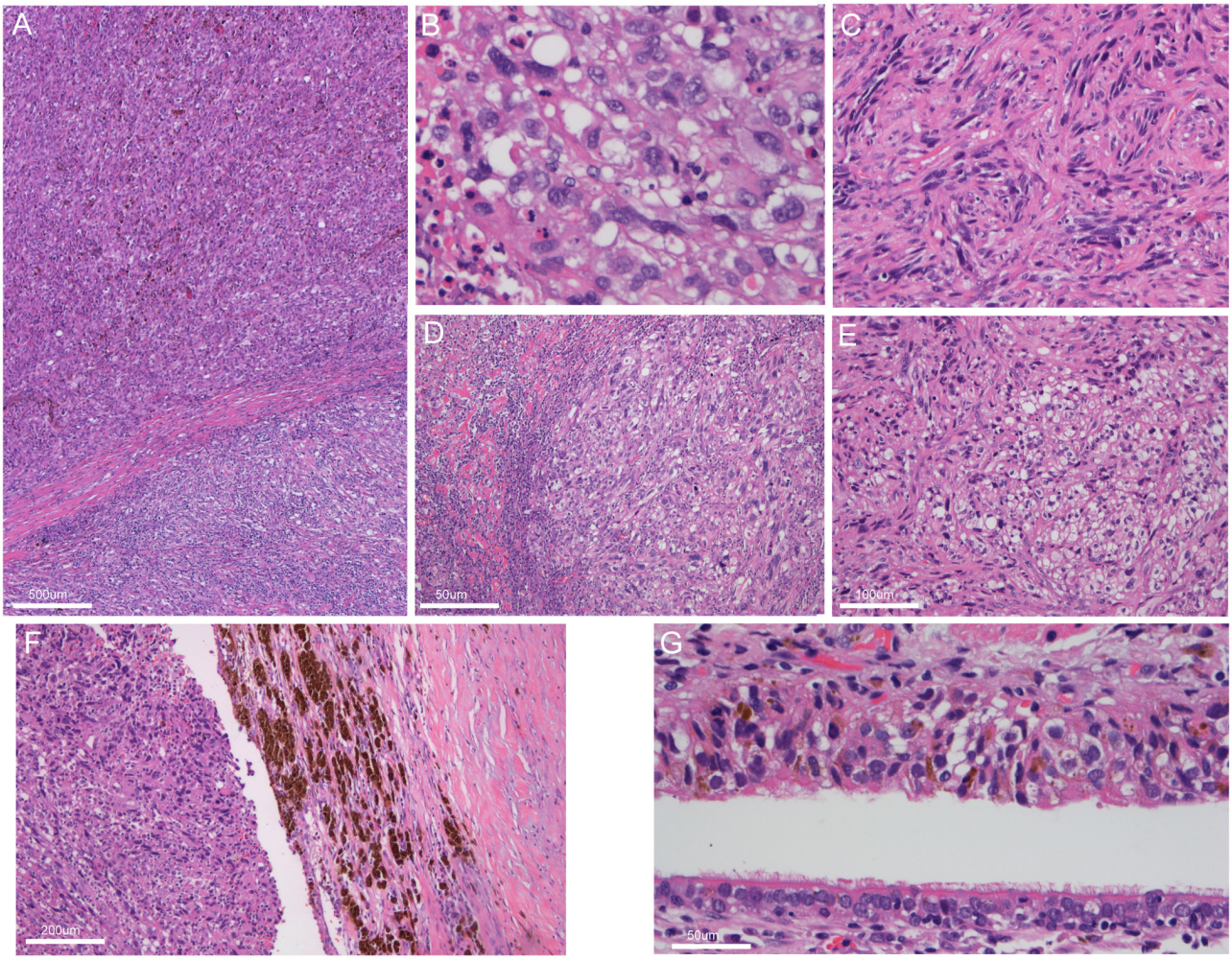

Figure 2. Histological features of primary pulmonary malignant melanoma (hematoxylin and eosin staining). (A) The tumor exhibited a nodular appearance with a relatively clear boundary, indicating infiltrative growth (x40 magnification). Biphasic differentiation was observed, with both (B) epithelioid cells and (C) spindle-shaped cells present (x400 magnification). Tumor cells exhibited (D) notable atypia, with bizarre morphology (x200 magnification), and (E) eosinophilic or transparent cytoplasm was commonly seen (x200 magnification). (F) There was a marked accumulation of melanin pigmentation in the tumor (x100 magnification). (G) Scattered or nest-like melanoma cells were observed beneath the bronchial mucosal epithelium, with no ulceration in the infiltrated bronchial mucosa (x400 magnification).

examinations, often appearing as solitary lung nodules on imaging (1).

Histologically, pPMM shares feature with melanomas from skin or mucosal sites, including epithelioid and spindle-shaped cells with significant nuclear atypia and melanin deposits. Distinguishing between pPMM and metastatic melanoma can be challenging due to the tendency of skin melanomas to degenerate after metastasis (7). The accurate diagnosis of pPMM requires a thorough evaluation of clinical, imaging and pathological findings. Previous studies (8,9) have proposed specific criteria for diagnosing pPMM. Jensen and Egedorf (8) suggested the following six criteria: i) No prior skin tumors removed; ii) no prior ocular tumors removed; iii) a solitary lung tumor; iv) morphology consistent with a primary tumor; v) no involvement of other organs; and vi) absence of primary MM demonstrated in other organs, particularly in the skin or eyes, confirmed by biopsy. According to the pathological diagnostic criteria for pPMM by Allen and Drash (9), the diagnosis of MM is based on bronchial epithelium invasion by melanoma cells,

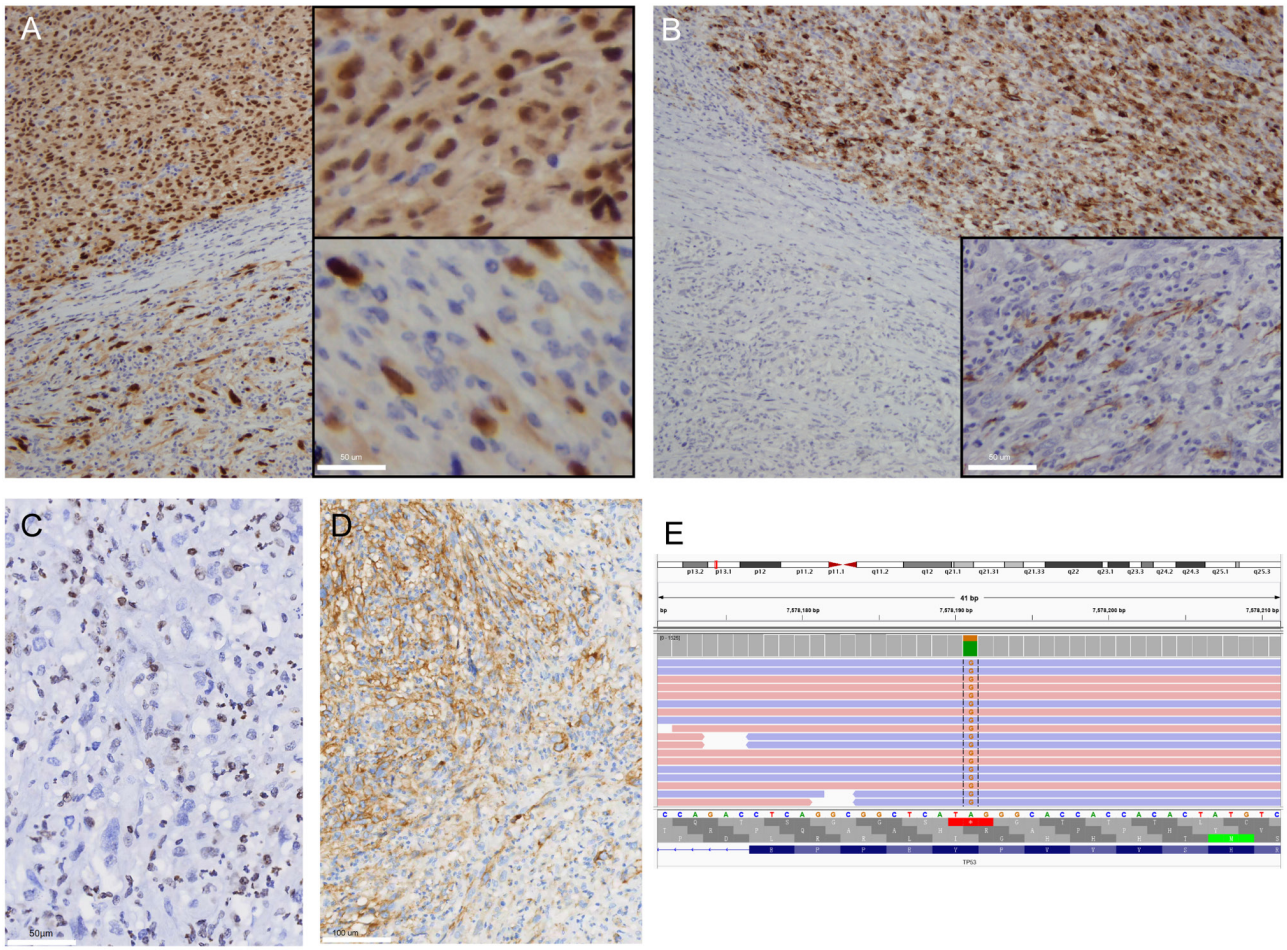

Figure 3. Histological and molecular features of primary pulmonary malignant melanoma. Immunohistochemical staining showed positive expression of melanoma markers, including (A) transcription factor SOX-10 and (B) Melan-A, with significantly stronger expression intensity in epithelioid regions compared with spindle cell regions (x40 magnification). (C) H3K27Me3 expression was lost in the tumor cell s (x400 magnification). (D) The programmed death-ligand 1 (SP263) positive rate was 60% (x200 magnification). (E) Integrative Genomics Viewer screenshot, highlighting the *TP53* gene mutation detected by next-generation sequencing.

junctional changes such as 'dropping off' or 'nesting' just beneath the bronchial epithelium, and confirmation of melanoma cells through immunohistochemical staining (S-100, HMB-45 and Melan-A) or electron microscopy. The present case met all these clinical and pathological criteria, leading to a diagnosis of pPMM.

The key differential diagnosis in the present case was MPNST, due to the rare presentation of MM in the pulmonary region, and as both MPNST and MM can exhibit melanin deposits and similar morphological features, making differentiation difficult (10,11). The biphasic differentiation in the present case, with both epithelioid and spindle cell characteristics, added complexities to the diagnosis. H3K27Me3 is a crucial epigenetic marker of gene silencing, intricately associated with heterochromatic regions; it plays a significant role in inflammation, DNA damage repair, cell proliferation, metastasis, regulatory cell death, ferroptosis and angiogenesis, thereby influencing various epigenetic mechanisms in the pathogenesis of multiple cancer types, such as glioblastoma (2). H3K27me3 is frequently observed to be lost in MPNST (3) and has also been documented in MM (12), indicating that this marker alone is insufficient to distinguish between the two. The correct identification of pPMM had significant clinical implications, as the treatment strategies for MM and MPNSTs differ substantially. Accurate diagnosis enabled the initiation of appropriate therapy, including targeted and immune-based treatments tailored to MM, which contributed to an improved clinical outcome for the patient. Differentiation from other malignancies, such as pulmonary sarcomatoid carcinoma, epithelioid inflammatory myofibroblastic sarcoma, angiosarcoma and leiomyosarcoma, is also crucial. Negative immunohistochemical markers for AE1/AE3, EMA, SMA, ALK and others helped rule out these diagnoses in the present study.

Genomic analysis of this pPMM revealed mutations similar to those found in mucosal and esophageal melanomas, contrasting with the common mutations seen in skin melanoma (13-15). In the present patient, NGS identified mutations in *TP53*, *NTRK3*, *NF1* and *BCL2L11*, while *BRAF* and *KIT* mutations, typically associated with skin melanoma, were absent. Research indicates that *NF1* mutations are prevalent in primary esophageal melanomas (13), supporting the idea that different anatomical locations may have distinct mutational profiles.

The prognosis for patients with pPMM is generally poor (4). However, the present patient has achieved long-term

disease-free survival for 72 months, possibly indicating a potential cure following surgical resection. This favorable outcome may be attributed to the incidental nature of the diagnosis, absence of clinical symptoms, early detection and H3K27Me3 loss, which has been suggested in previous studies to correlate with a more favorable prognosis in melanoma (16,17). High H3K27Me3 expression is associated with more aggressive melanoma cell phenotype and poorer outcomes (18), emphasizing the significance of this biomarker in assessing melanoma prognosis and possible therapeutic approaches based on the gennomic findings.

There are some limitations to the present study. The report is based on a single case, which limits the generalizability of the findings and the exploration of potential treatment strategies for pPMM. Given the rarity of the condition, discussing possible treatment options based on the genomic findings would have been beneficial. Therefore, more cases are needed to validate the observations and conclusions in future studies.

In conclusion, the current study presents a rare case of pPMM, initially misdiagnosed as MPNST, characterized by H3K27me3 loss and a histological profile displaying both epithelial and spindle cell features. The case findings highlight the complexities involved in diagnosing pPMM and the critical importance of comprehensive clinical and pathological evaluation.

Acknowledgements

Not applicable.

Funding

The present study was supported by Fujian Provincial Natural Science Foundation (grant no. 2024J011006) and Fujian Provincial Science and Technology Innovation Joint Funds (grant no. 2024Y96010076).

Ethics approval and consent to participate

The Ethics Committee of Fujian Provincial Hospital (Fuzhou, China) approved the present study (approval no. K2024-09-070) and waived the requirement for informed consent. The present study was performed in accordance with the principles of the Declaration of Helsinki.

Availability of data and materials

The data generated in the present study may be found in the SRA database under accession number PRJNA1245001 or at the following URL: https://www.ncbi.nlm.nih.gov/sra/?term=PRJNA1245001. All other data generated in the present study may be requested from the corresponding author.

Authors' contributions

HL and LZ conceived and designed the experiments. HL, LZ, XY, LC and SL performed the experiments. HL, XY, LC, SL and XC analyzed the data. HL, LZ and XC provided the reagents, materials and/or the analysis tools. HL and LZ confirm the authenticity of all the raw data. HL and LZ wrote the paper. All authors have read and approved the final manuscript.

Patient consent for publication

The patient provided written informed consent for publication of their data.

Competing interests

The authors declare that they have no competing interests.

References

1. Kyriakopoulos C, Zarkavelis G, Andrianopoulou A, Papoudou-Bai A, Stefanou D, Boussios S and Pentheroudakis G: Primary pulmonary malignant melanoma: Report of an important entity and literature review. Case Rep Oncol Med 2017: 8654326, 2017.
2. Di L and Zhu WG: The role of H3K27me3 methylation in cancer development. Genome Instab Dis 5: 17-34, 2024.
3. Cortes-Ciriano I, Steele CD, Piculell K, Al-Ibraheemi A, Eulo V, Bui MM, Chatzipli A, Dickson BC, Borcherding DC, Feber A, *et al*: Genomic patterns of malignant peripheral nerve sheath tumor (MPNST) evolution correlate with clinical outcome and are detectable in cell-free DNA. Cancer Discov 13: 654-671, 2023.
4. Li H, Zheng L, Zhang X, Yu X, Zhong G, Chen X, Chen X and Chen L: SH3 domainbinding glutamic acidrich protein-like 3 is associated with hyperglycemia and a poor outcome in EpsteinBarr virusnegative gastric carcinoma. Oncol Lett 29: 8, 2024.
5. Zhu Z, Dong H, Wu J, Dong W, Guo X, Yu H, Fang J, Gao S, Chen X, Lu H, *et al*: Targeted genomic profiling revealed a unique clinical phenotype in intrahepatic cholangiocarcinoma with fibroblast growth factor receptor rearrangement. Transl Oncol 14: 101168, 2021.
6. Shi Y, Bing Z, Xu X and Cui Y: Primary pulmonary malignant melanoma: Case report and literature review. Thorac Cancer 9: 1185-1189, 2018.
7. Kamposioras K, Pentheroudakis G, Pectasides D and Pavlidis N: Malignant melanoma of unknown primary site. To make the long story short. A systematic review of the literature. Crit Rev Oncol Hematol 78: 112-126, 2011.
8. Jensen OA and Egedorf J: Primary malignant melanoma of the lung. Scand J Respir Dis 48: 127-135, 1967.
9. Allen MS Jr and Drash EC: Primary melanoma of the lung. Cancer 21: 154-159, 1968.
10. Gaspard M, Lamant L, Tournier E, Valentin T, Rochaix P, Terrier P, Ranchere-Vince D, Coindre JM, Filleron T and Le Guellec S: Evaluation of eight melanocytic and neural crest-associated markers in a well-characterised series of 124 malignant peripheral nerve sheath tumours (MPNST): Useful to distinguish MPNST from melanoma?. Histopathology 73: 969-982, 2018.
11. Hrycaj SM, Szczepanski JM, Zhao L, Siddiqui J, Thomas DG, Lucas DR, Patel RM, Harms PW, Bresler SC and Chan MP: PRAME expression in spindle cell melanoma, malignant peripheral nerve sheath tumour, and other cutaneous sarcomatoid neoplasms: A comparative analysis. Histopathology 81: 818-825, 2022.
12. Le Guellec S, Macagno N, Velasco V, Lamant L, Lae M, Filleron T, Malissen N, Cassagnau E, Terrier P, Chevreau C, *et al*: Loss of h3k27 trimethylation is not suitable for distinguishing malignant peripheral nerve sheath tumor from melanoma: A study of 387 cases including mimicking lesions. Mod Pathol 30: 1677-1687, 2017.
13. Tsuyama S, Kohsaka S, Hayashi T, Suehara Y, Hashimoto T, Kajiyama Y, Tsurumaru M, Ueno T, Mano H, Yao T and Saito T: Comprehensive clinicopathological and molecular analysis of primary malignant melanoma of the oesophagus. Histopathology 78: 240-251, 2021.

14. Li J, Guan W, Ren W, Liu Z, Wu H, Chen Y, Liu S, Quan X, Yang Z, Jiang C, *et al*: Longitudinal genomic alternations and clonal dynamics analysis of primary malignant melanoma of the esophagus. Neoplasia 30: 100811, 2022.
15. Tímár J and Ladányi A: Molecular pathology of skin melanoma: Epidemiology, differential diagnostics, prognosis and therapy prediction. Int J Mol Sci 23: 5384, 2022.
16. Hou C, Xiao L, Ren X, Cheng L, Guo B, Zhang M and Yan N: EZH2-mediated H3K27me3 is a predictive biomarker and therapeutic target in uveal melanoma. Front Genet 13: 1013475, 2022.
17. Luo C, Balsa E, Perry EA, Liang J, Tavares CD, Vazquez F, Widlund HR and Puigserver P: H3K27me3-mediated PGC1α gene silencing promotes melanoma invasion through WNT5A and YAP. J Clin Invest 130: 853-862, 2020.
18. Hoffmann F, Niebel D, Aymans P, Ferring-Schmitt S, Dietrich D and Landsberg J: H3K27me3 and EZH2 expression in melanoma: Relevance for melanoma progression and response to immune checkpoint blockade. Clin Epigenetics 12: 24, 2020.